LOCAL STRUCTURE OF LIQUID ZIRCONIUM: MOLECULAR DYNAMICS STUDY

Sedat SENGUL, Unal DOMEKELI
Faculty of Science, Trakya University, Edirne, Turkey

Abstract

Zirconium (Zr) and its alloys are widely-used structural materials in the nuclear power plant industry as reactor core structural materials for their good mechanical strength and low neutron absorption. We present molecular dynamics simulations of the thermodynamic melting transition of hcp Zr, using well-known formulation of embedded atom potentials to define the interactions between Zr atoms. We studied various low and high temperature properties such as cohesive energy, pair distribution function, melting temperature, of Zr. The results were discussed in terms of possible experimental and/or theoretical data.

Keywords: Zirconium, embedded atom potentials, molecular dynamics simulations, pair distribution functions

INTRODUCTION

Zirconium (Zr) and its alloys have technical applications in aerospace, medical fields due to its light weight and corrosion resistance [1,2]. Zr element has the hexagonal close-packed (hcp) structure (or α- phase) at ambient conditions. It was reported that its structure transforms to the body-centered cubic (bcc) structure [3].

Zr has been the subject of many theoretical studies to develop many-body interatomic potentials for the hcp structures of various materials, especially for Zr. Molecular Dynamics (MD) simulations are a powerful tool to investigate time evolution and local structure of materials in terms of positions of the atoms [4,5], due to their ability to provide atomic-level information. The defining the interatomic interactions strongly affects the success of MD simulations. Previous MD simulation studies [6,7] of Zr were conducted mainly by using the embedded-atom method (EAM) potential developed by Ackland et al. [8], which is known to have the limitation of calculating stacking fault energies using ab initio calculations. Recently, Zhou et al. [9] (EAM1) and Cheng et al. [10] (EAM2) parameterized EAM potentials for pure Zr and some multicomponent Zr alloys. In our previous studies we were interested in glass formation process of Zr based binary [11,12] and ternary alloys [13–15]. In this work, as a case study, we were interested in the properties of solid and liquid Zr. We re-calculated some fundamental properties of solid and liquid Zr using well-known EAM potentials (denoted as EAM1 and EAM2) to define the interactions between Zr atoms, and compare them with available experimental data. Our aim was to test most – used set of EAM potentials [9,10] for Zr and verify which one is useful for nano-scale calculation on Zr.

EXPOSITION

The reliability of an MD simulation depends on the interatomic potential to explain the atomic interactions of a system. The EAM potential consists of simple embedding energy functions and pair potential functions, and can be expressed as:

$$E_i = F_i(\rho_i(r)) + \frac{1}{2}\sum_{j\neq i}\phi(r) \qquad (1)$$

where r is the distance between atoms, and $\phi(r)$, $\rho(r)$, and F are the pair, density, and embedded functions, respectively. There is more detailed information about these three functions in Ref.[16].

The MD simulations were performed by using large-scale atomic/molecular massively

parallel simulator (LAMMPS)[17] based on EAM potential. The simulation box was a hexagonal with 16384 Zr atoms. Periodic boundary conditions were applied all directions. The NPT canonical ensemble was applied and the time step is 1 fs. The initial configuration was constructed as hcp lattice with experimental values of a_o= 3.231 Å and c_0 = 5.148 Å[18]. Crystalline lattice equilibrated at zero temperature to calculate cohesive energy for 0.6 ns. Then, the system heated up to room temperature to calculate equilibrium lattice structure with 1 ns. The equilibrated system was heated up to 2500 K with the heating rate of 2.5 10^{12} K/s.

To test the validity of EAM potentials for hcp-Zr, the atomic energies for atomic volumes near equilibrium state were calculated. Figure 1 compares the results of calculations. We point out that the equilibrium atomic volume for hcp Zr obtained by EAM1 is slightly different from the one obtained by EAM2. Table 1 lists simulated solid state properties of hcp Zr. The agreement in terms of the equilibrium lattice parameter is remarkable. There is fair agreement for the cohesive energies both experiment and simulations. For the cohesive energies, although its value for EAM1 is slightly larger than that of experimental, for hcp crystalline state, it appears that EAM1 more stable than EAM2. The results demonstrate that both EAM potentials can describe the properties of hcp Zr, quite well, including the ground state properties, as well as in terms of cohesive energy.

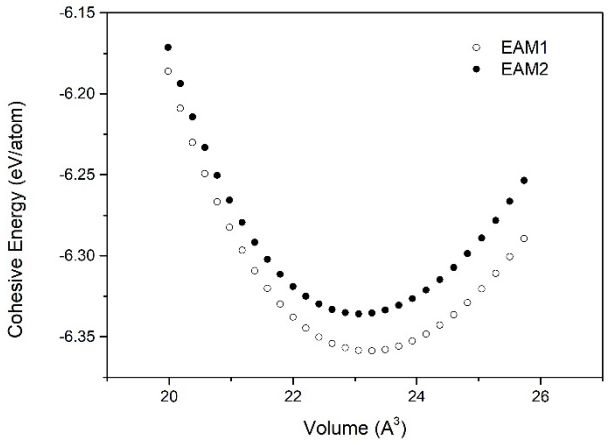

Fig. 1. *Cohesive energy as a function of atomic volume for hcp Zr*

We also calculated the elastic constants and bulk modulus for hcp Zr. There is reasonable agreement between our results and experimental data, except for melting temperature, T_m. The melting point is defined as the temperature at which the solid and liquid phases of a material exist simultaneously. At the melting point, the system lacks metallic bonds and this is indicated by a sharp increase in the caloric curve during heating. Figure 2 plots the temperature dependence of potential energy for hcp Zr during heating. Although EAM1 and EAM2 successively produce the solid state properties, EAM2 produces lower melting point for hcp Zr than experiment and EAM1. It means that EAM1 is suitable for studying the properties at higher temperatures.

Table 1*. Simulated lattice properties of hcp Zr*

	EAM1	EAM2	**Exp.**
a_o (Å)	3.227	3.227	3.231[a]
c_o (Å)	5.143	5.138	5.148[a]
E_0(eV/atom)	-6.32	-6.35	-6.32[a]
B(10^{11} Pa)	0.807	0.847	0.976[a]
c_{11}(GPa)	103.49	101.45	144[b]
c_{12}(GPa)	65.55	115.21	74[b]
c_{13}(GPa)	58.82	46.10	67[b]
c_{33}(GPa)	153.26	144.42	166[b]
c_{44}(GPa)	28.24	28.33	33[b]
T_m(K)	2160	1720	2123

[a]Ref.[18]
[b]Ref.[19]

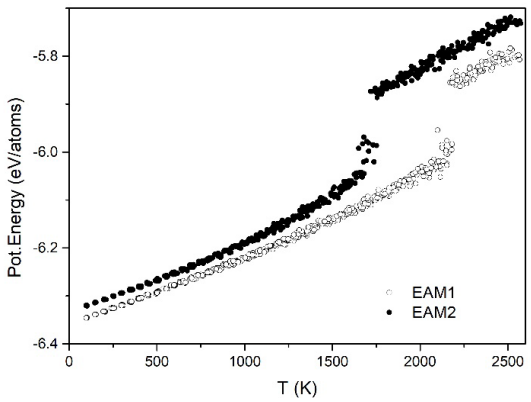

Fig. 2. *Potential energy as a function of temperature during heating of hcp Zr*

The pair distribution function, g(r) showing the probability of finding another atom at a distance r from an origin atom, is used to characterize the structural properties of liquids and noncrystalline solids, and is defined as

$$g(r) = \frac{V}{4\pi r^2 N^2} \langle \sum_{i}^{N} \sum_{j \neq i}^{N} \delta(r) \rangle \qquad (2)$$

where N is the number of atoms in the system, V is the volume of simulation box, $\delta(r-r_{ij})$ is the Dirac delta function, and the angular brackets represent a time average. Figure 3 (a, b) display obtained g(r)' for hcp Zr at different temperatures using EAM1 and EAM2 potential sets, respectively. At room temperature, g(r)s from both sets of EAM have sharp and narrow peaks which denotes crystalline long range order. In terms of the peak positions, the behavior of g(r)s indicates a typical hcp crystalline order at 300 K. The nearest neighbor distance remains almost unchanged, and peaks become broader and shallower with increasing temperature, which is an indication that the atomic ordering in the first coordination shell decreases. Further increasing temperature, minor-peaks disappeared and g(r)s have an obvious first peak, visible second peak and featureless tail meaning firs-order phase transition. The broadening of major peaks and the disappearing of minor peaks of g(r) are characteristic of liquids. After melting is complete, the minor peaks vanishes at a temperature of 2200 K and 1790 K for EAM1 and EAM2, respectively.

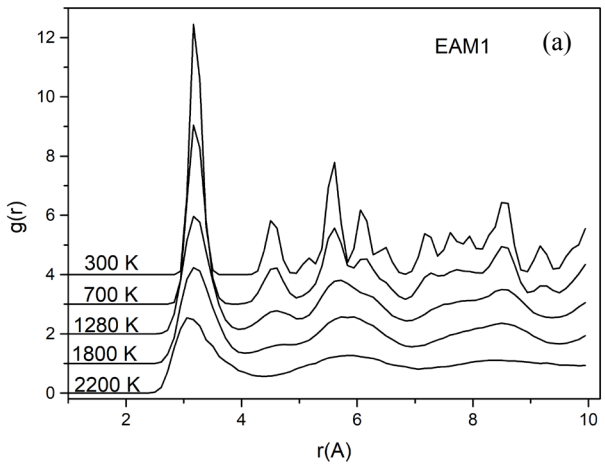

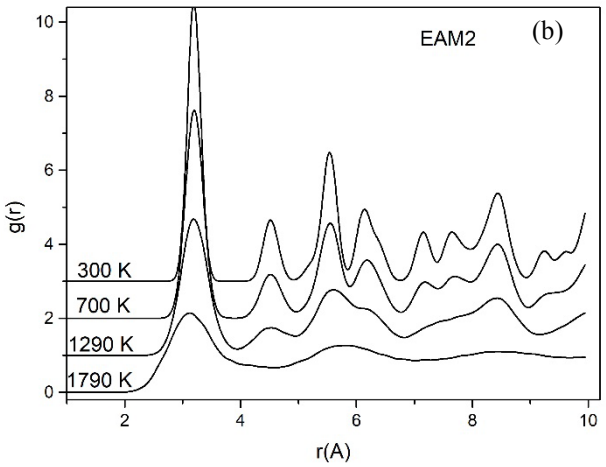

Fig. 3. *Pair distribution functions calculated by a) EAM1 b) EAM2 for hcp Zr*

CONCLUSION

In this paper, we have re-calculated the solid and liquid state properties of hcp Zr by molecular dynamics simulations in which interactions defined by means of EAM potentials parameterized by Zhou et al.[9] and Cheng et al.[10]. We observed that both EAM sets successfully produce the properties at room temperature in terms of cohesive energy, lattice parameters and elastic constants. Only difference is at the melting temperature of hcp Zr. The melting temperature obtained by EAM1 set parameterized by Zhou et al. is in fair agreement with experimental. We can conclude that their parameterization can be used to study the properties of Zr at high temperatures, and useful for nano-scale calculations.

REFERENCE

[1] Y.K. Vohra, P.T. Spencer, Novel γ-Phase of Titanium Metal at Megabar Pressures, Phys. Rev. Lett. 86 (2001) 3068–3071. doi:10.1103/PhysRevLett.86.3068.

[2] C. Yan, R. Wang, Y. Wang, X. Wang, G. Bai, Effects of ion irradiation on microstructure and properties of zirconium alloys—A review, Nucl. Eng. Technol. 47 (2015) 323–331. doi:10.1016/J.NET.2014.12.015.

[3] Y. Ouyang, J. Wu, M. Zheng, H. Chen, X. Tao, Y. Du, Q. Peng, An interatomic potential for simulation of defects and phase change of zirconium, Comput. Mater. Sci. 147 (2018) 7–17. doi:10.1016/j.commatsci.2018.01.049.

[4] K. Nordlund, M. Ghaly, R.S. Averback, M. Caturla, T. Diaz de la Rubia, J. Tarus, Defect production in collision cascades in elemental semiconductors and fcc metals, Phys. Rev. B. 57 (1998) 7556–7570. doi:10.1103/PhysRevB.57.7556.

[5] D.J. Bacon, F. Gao, Y.N. Osetsky, The primary damage state in fcc, bcc and hcp metals as seen in molecular dynamics simulations, J. Nucl. Mater. 276 (2000) 1–12. doi:10.1016/S0022-3115(99)00165-8.

[6] S.. Wooding, L.. Howe, F. Gao, A.. Calder, D.. Bacon, A molecular dynamics study of high-energy displacement cascades in α-zirconium, J. Nucl. Mater. 254 (1998) 191–204. doi:10.1016/S0022-3115(97)00365-6.

[7] F. Gao, D.J. Bacon, L.M. Howe, C.B. So, Temperature-dependence of defect creation and clustering by displacement cascades in α-zirconium, J. Nucl. Mater. 294 (2001) 288–298. doi:10.1016/S0022-3115(01)00483-4.

[8] G.J. Ackland, S.J. Wooding, D.J. Bacon, Defect, surface and displacement-threshold properties of α-zirconium simulated with a many-body potential, Philos. Mag. A. 71 (1995) 553–565. doi:10.1080/01418619508244468.

[9] X.W. Zhou, R.A. Johnson, H.N.G. Wadley, Misfit-energy-increasing dislocations in vapor-deposited CoFe/NiFe multilayers, Phys. Rev. B. 69 (2004) 144113.

[10] Y.Q. Cheng, E. Ma, H.W. Sheng, Atomic Level Structure in Multicomponent Bulk Metallic Glass, Phys. Rev. Lett. 102 (2009) 245501. doi:10.1103/PhysRevLett.102.245501.

[11] M. Celtek, S. Sengul, Thermodynamic and dynamical properties and structural evolution of binary Zr80Pt20 metallic liquids and glasses: Molecular dynamics simulations, J. Non. Cryst. Solids. 498 (2018) 32–41. doi:10.1016/J.JNONCRYSOL.2018.06.003.

[12] M. Celtek, S. Sengul, U. Domekeli, C. Canan, Molecular dynamics study of structure and glass forming ability of Zr70Pd30 alloy, Eur. Phys. J. B. 89 (2016) 65–65. doi:10.1140/epjb/e2016-60694-5.

[13] S. Sengul, M. Celtek, U. Domekeli, Molecular dynamics simulations of glass formation and atomic structures in Zr60Cu20Fe20 ternary bulk metallic alloy, Vacuum. 136 (2017) 20–27. doi:10.1016/j.vacuum.2016.11.018.

[14] M. Celtek, S. Sengul, The characterisation of atomic structure and glass-forming ability of the Zr–Cu–Co metallic glasses studied by molecular dynamics simulations, Philos. Mag. (2018). doi:10.1080/14786435.2018.1425012.

[15] M. Celtek, S. Sengul, U. Domekeli, Glass formation and structural properties of Zr50Cu50-xAlx bulk metallic glasses investigated by molecular dynamics simulations, Intermetallics. 84 (2017) 62–73. doi:10.1016/j.intermet.2017.01.001.

[16] M.S. Daw, M.I. Baskes, Embedded atom method: derivation and application to impurities,surfaces and other defects in metal, Phys. Rev. B. 29 (1984) 6443–6453.

[17] S. Plimpton, Fast Parallel Algorithms for Short-Range Molecular Dynamics, J. Comput. Phys. 117 (1995) 1–19. doi:10.1006/JCPH.1995.1039.

[18] O. B, J.C. Jamieson, Zirconium: pahses and compressibility to 120 kilobars, High Temp.-High Press. 5 (1973) 123–131.

[19] E.A. Brandes, Smithells Metals Reference Book, London:Butterword, 1983.